Nonsynchronous Modes and Bifurcation of a Frequency-Phase-Feedback Oscillator with an Inverted Frequency Discriminator Characteristic

Valery P. Ponomarenko

Research Institute of Applied Mathematics and Cybernetics,
Nizhni Novgorod, Russia, povp@uic.nnov.ru

Abstract

The results of a numerical investigation of dynamical states and bifurcation transitions of a frequency-phase-feedback oscillator models with an inverted frequency discriminator characteristic are presented in the paper. The behavior of the examined models is described by nonlinear two- and five-dimensional set of differential equations with periodical nonlinearities. It is shown that the models demonstrate complex behavior including chaotic self-modulation oscillations. Results are presented using a two-parameter portrait of motions, one-parameter bifurcation diagrams, and phase portraits of attractors.

I. Introduction

In recent years a great interest has been devoted to the study of complex dynamics phenomena in the systems with phase and frequency control. Such systems are traditionally intended to provide for and maintain the synchronous state, when the phase difference of reference and controlled signals becomes constant or, equivalently, the frequency difference of these signals is equal to zero [1]. The systems may also operate in nonsynchronous modes with variable phase and frequency errors. The use of such modes opens wide possibilities for some nontraditional engineering and technological applications of phase- and frequency-control systems (generation of complex periodic and chaotic signals, oscillation control, data transmission and processing, etc.).

The purpose of this paper is to present new results concerning the nonsynchronous states of system with frequency-phase control combining phase-lock (PL) and frequency-lock (FL) systems. The system incorporates the controlled oscillator with two feedback loops including nonlinear discriminators of phase and frequency errors, low-frequency filters (LFFs) with transfer functions $K_1(p)$ and $K_2(p)$, and a frequency modulator. We investigate nonlinear dynamics and nonsynchronous modes of the frequency-phase lock (FPL) system with an inverted frequency discriminator characteristic in two cases: when each separate system demonstrates regular dynamics and when, the PL subsystem autonomously exhibits only regular behavior, whereas an isolated FL subsystem may operate in both regular and chaotic nonsynchronous modes. Using frequency discriminator with inverted characteristic open new possibilities of forming nonsynchronous modes in FPL system, which we would like to discuss below. On the basis of qualitative-numerical analysis, we found the parameter regions corresponding to monoharmonic, periodic and chaotic automodulation regimes of controlled oscillator.

II. FPL system models under consideration

Equations describing the dynamics of the considered FPL system can be represented in the following operator form ($p\equiv d/dt$) [2,3]:

$$p\varphi+\Omega K_1(p)F(\varphi)-\Omega_1 K_2(p)\Phi(p\varphi)=\delta\omega, \qquad (1)$$

where φ is the phase difference between the reference and controlled signals; $F(\varphi)$ and $\Phi(p\varphi)$ are the characteristics of phase and frequency discriminators normalized to unity; Ω and Ω_1 are the control circuit gains; and $\delta\omega$ is the initial frequency mistuning. Sign "minus" before Ω_1 corresponds to inverting frequency discriminator characteristic. Assume that the functions $F(\varphi)=\sin\varphi$ and $\Phi(p\varphi)=2\beta_1 p\varphi/(1+\beta_1^2(p\varphi)^2)$ (β_1^{-1} is the frequency mistuning providing for the maximum value of $\Phi(p\varphi)$) approximate the phase and frequency discriminator characteristics respectively.

Consider the simplest first-order filters with transfer functions $K_1(p)=1$, $K_2(p)=1/(1+b_1 p)$, where b_1 is the inertia parameter. Equations (1) may be written in this case as

$$d\varphi/d\tau=\eta,\ d\eta/d\tau=\gamma-\sin\varphi+b\Phi(\beta\lambda\eta)-(\lambda+\lambda^{-1}\cos\varphi)\eta, \qquad (2)$$

where $\tau=(\Omega_1/b_1)^{1/2}t$ is the dimensionless time, $\lambda=1/(\Omega_1 b_1)^{1/2}$), $\gamma=\delta\omega/\Omega_1$, $\Phi(\beta\lambda\eta)=2\beta\lambda\eta/(1+\beta^2\lambda^2\eta^2)$, $b=\Omega_2/\Omega_1$, $\beta=\beta_1\Omega_1$. The system (2) is considered on the cylindrical phase surface $U_0=\{\varphi(mod\,2\pi),\eta\}$.

Now consider the first-order filter in PL subsystem and third-order filter in FL subsystem with transfer functions $K_1(p)=1/(1+b_0 p)$, $K_2(p)=1/(1+b_1 p+b_2 p^2+b_3 p^3)$, where b_0, b_1, b_2, and b_3 are the inertia parameters. In this case, the system of equations is written as

$$\begin{aligned} &d\varphi/d\tau=u,\quad du/d\tau=z,\quad dz/d\tau=v,\quad dv/d\tau=w,\\ &\varepsilon_1\mu_2\, dw/d\tau=\gamma-\sin\varphi-b\Phi(y)-(1+\varepsilon_2\cos\varphi)u-(\varepsilon_1+\varepsilon_2+\\ &+\mu_1\cos\varphi+b\beta\varepsilon_1\Phi'(y))z-(\mu_1+\mu_2\cos\varphi+\varepsilon_1\varepsilon_2)v-\\ &-(\mu_1\varepsilon_1+\mu_2)w+\mu_1 u^2\sin\varphi+\mu_2 u^3\cos\varphi+3\mu_2 uz\sin\varphi, \end{aligned} \qquad (3)$$

where $\tau=\Omega t$, $\varepsilon_1=b_0\Omega_1$, $\varepsilon_2=b_1\Omega_1$, $\mu_1=b_2\Omega_1^2$, $\mu_2=b_3\Omega_1^3$, $\Phi(y)=2y/(1+y^2)$, $\Phi'(y)=2(1-y^2)/(1+y^2)^2$, $y=\beta u$. System

(3) has the cylindrical phase space $U=\{\varphi(mod\ 2\pi),u,z,v,w\}$.

Since systems (2) and (3) are nonlinear, its nonlocal investigation encounters serious difficulties. Therefore, we apply computer simulation based on qualitative-numerical methods of analysis of nonlinear dynamical systems [4,5] and employ the software developed in [6].

III. Dynamical states of model (2)

At $0\le\gamma<1$, system (2) has two equilibrium states: $A_1(arcsin\gamma,\ 0)$ and $A_2(\pi-arcsin\gamma,\ 0)$. The equilibrium state A_1 is stable for $b<b_s$ and unstable for $b>b_s$, where $b_s=(1+(1-\gamma^2)^{1/2}/\lambda^2)/2\beta$, whereas the equilibrium state A_2 is unstable of saddle type. The stable equilibrium state A_1 corresponds to synchronous mode of the FPL system. The results obtained in [7] show that the system (2) has no limit cycles when $b\le0$, $0\le\gamma<1$, its phase portrait is given in Fig.1a. In this case synchronous mode is realized in the FPL system irrespective of initial conditions.

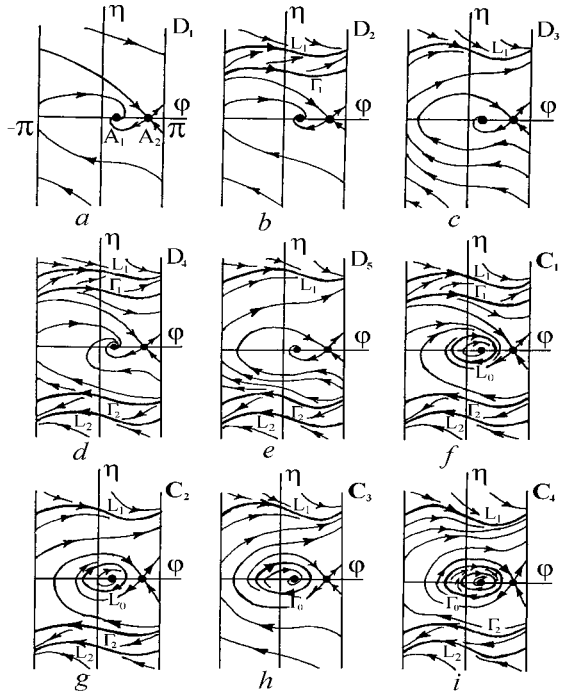

Fig. 1. Phase portraits of model (2) for domains D_1–D_5, and C_1–C_4

Here we consider dynamic processes evolving in model (2) for $b>0$ when parameter γ and b vary and the remaining parameters are fixed. Fig.2 shows disposition of bifurcation curves on the (γ,b) plane, calculated at $\lambda=0.2$, $\beta=4.0$. Line 1 corresponds to saddle A_2 separatrix loop Π_0 of the first kind that is not encompasses the phase cylinder U_0. The loop Π_0 is unstable as the saddle value $\sigma=(2\beta b-1)\lambda+(1-\gamma^2)^{1/2}/\lambda>0$. Upon passing throw line 1, as b is increased, an unstable oscillatory type limit cycle Γ_0 such that a phase difference φ varies within a limited range not exceeding 2π appears on the phase cylinder U_0.

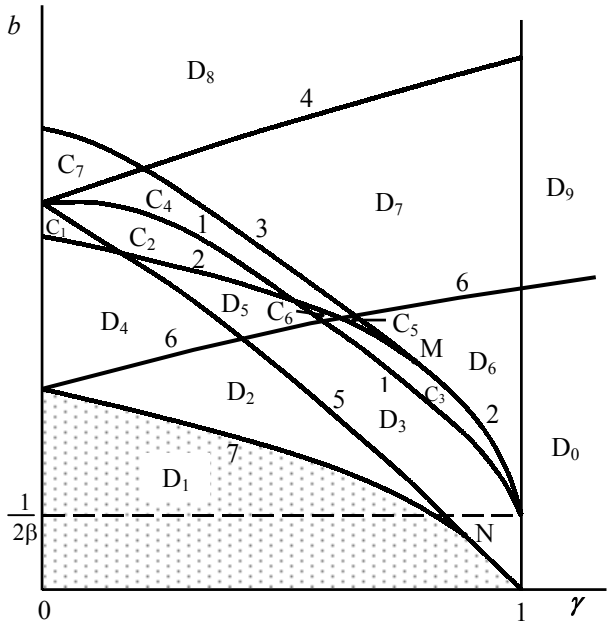

Fig. 2. Dynamic mode domains for model (2)

Line 2 is a stability boundary b_s of the equilibrium state A_1. We investigated the behavior of the model (2) at the boundary b_s by analyzing the first Lyapunov value $L=-\pi\{6\beta^2\lambda^2(1-\gamma^2)(\lambda^2+(1-\gamma^2)^{1/2})-1\}/(8\lambda(1-\gamma^2)^{3/4})$. It was found that the part b_s^- of curve b_s above the point M is a safe stability boundary ($L<0$), whereas the part b_s^+ of curve b_s below the point M is unsafe stability boundary ($L>0$). Note, that the point M corresponds to $\gamma=\gamma^0=(1-(1/2+\beta^2/6-(1/4+\beta^2/6)^{1/2})/\lambda^4)^{1/2}$. Therefore, upon passing through the curve b_s^-, as b is increased, a stable oscillatory type limit cycle L_0 occurs around equilibrium state A_1 that has become unstable. Cycle L_0 corresponds to a quasi-synchronous mode in the FPL system when periodic oscillations of errors φ and η are observed around equilibrium state A_1. Upon passing through the curve b_s^+, as b is increased, an unstable limit cycle Γ_0 vanishes transforming into equilibrium state A_1.

Line 3 corresponds to double (saddle-node) limit cycle of oscillatory type. Upon passing through the line 3, as b is increased, limit cycles L_0 and Γ_0 merge and disappear.

Bifurcation curves 4 and 5 correspond to saddle separatrix loops of the second rind (rotatory type): Π^- in the half phase cylinder $\eta<0$ and Π^+ in the half phase cylinder $\eta>0$ respectively, that encompass the phase cylinder U_0. The loop Π^+ is stable at the part of the curve 5 below the point N (where the saddle value $\sigma<0$) and unstable at the part of the curve 5 above the point N (where $\sigma>0$). Note, that the point N corresponds to $\gamma=\gamma_s=(1-\lambda^4(2\beta b-1)^2)^{1/2}$. Therefore, upon passing throw the curve 5, if b is increased and $\gamma>\gamma_s$, a stable rotatory type (2π-periodic in φ) limit cycle L_1 appears in the half phase cylinder $\eta>0$. Upon passing throw the curve 5, as b is decreased and $\gamma<\gamma_s$, an unstable rotatory type limit cycle Γ_1 appears in the half phase cylinder $\eta>0$. The separatrix loop Π^- is unstable as $\sigma>0$. When, as a re-

sult of diminishing b, the system (2) crosses line 4, an unstable rotatory type limit cycle Γ_2 appears in the half phase cylinder $\eta<0$.

Lines 6 and 7 correspond to double (saddle-node) rotatory type limit cycles in the half phase cylinder $\eta<0$ and $\eta>0$ respectively. If, as a result of increasing b, the system (2) crosses line 7, a stable rotatory type limit cycle L_1 and an unstable rotatory type limit cycle Γ_1 are born in the half phase cylinder $\eta>0$. Upon passing throw the line 6, as b is increased, a stable rotational limit cycle L_2 and an unstable rotational limit cycle Γ_2 appears in the half phase cylinder $\eta<0$. Cycles L_1 and L_2 are associated with the asynchronous modes of the FPL system such that phase error φ rotates and frequency error η periodically oscillate about certain mean value.

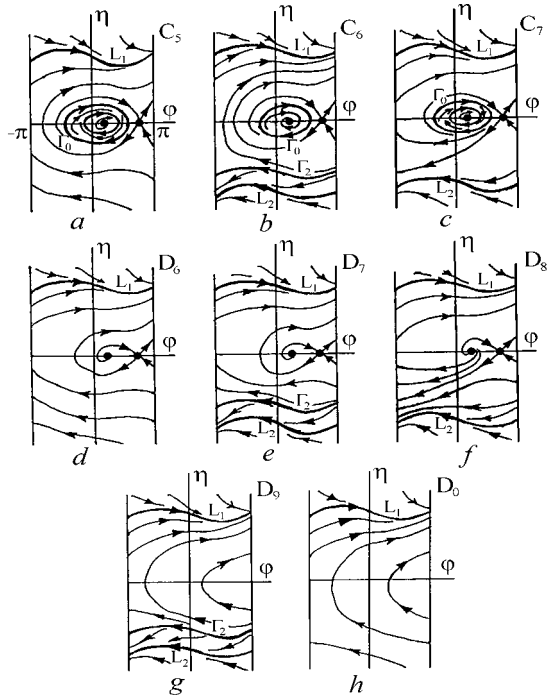

Fig.3 Phase portraits of model (2) for domains C_5–C_7, D_6–D_9, and D_0

Bifurcation curves 1-7 given at Fig.2 identify various parameter domains possessing qualitatively different dynamics of the model (2). Fig.1 and Fig.3 show the phase portraits of the system (2) for dynamic mode domains represented in Fig.2. For the parameters from domain D_1 there are no limit cycles and equilibrium state A_1 is the only attractor (Fig.1a). The trajectories on the phase cylinder U_0 converge to A_1 independently of initial state of the system. Therefore, when the values of parameters belong to domain D_1, the FPL system is in synchronous mode irrespective of the initial conditions. For the parameters from domains D_2,D_3,D_4,D_5,C_3, and C_6 a stable equilibrium state A_1 and stable limit cycles L_1 and L_2 are simultaneously exist on the phase cylinder U_0 (Figs.1b-1e, 1h, and 3b). Depending on initial conditions, synchronous or asynchronous mode corresponding to these attractors develops. When the parameter values belong to domains C_1, C_2,C_4,C_5,C_7,D_6,D_7, and D_8 quasi-synchronous mode with limit cycle L_0 or asynchronous modes with limit cycles L_1 and L_2 are realized in the FPL system (Figs.1f, 1g, 1i, 3a, and 3c-3f). In parameter domains D_9 and D_0 the system exhibits asynchronous modes with limit cycles L_1 and L_2 (Figs.3g, 3h). Note, that the regions of attraction of equilibrium state A_1 and limit cycles L_0, L_1, and L_2 are bounded by unstable limit cycles Γ_0, Γ_1, and Γ_2 and of saddle A_2 separatrix on the phase cylinder U_0.

From the results obtained in framework of model (2) we show that inverting of the frequency discriminator characteristic make possible the appearance in the FPL system of periodical auto modulation regimes corresponding to oscillatory and rotatory type limit cycles on the phase cylinder U_0 which are not possible in partial PL and FL systems.

IV. Peculiarities of nonsynchronous modes of model (3)

First, let us analyze the stability of the FPL system synchronous mode. The condition under which equilibrium state $A_1(arcsin\gamma, 0,0,0)$ is stable is determined by the following inequalities:

$$c_1c_2-c_3>0, \quad (c_1c_2-c_3)(c_3c_4-c_3c_5)-(c_1c_4-c_5)>0 \qquad (4)$$

where

$$c_1=(\mu_1\varepsilon_1+\mu_2)/(\mu_2\varepsilon_1),\ c_2=(\varepsilon_1\varepsilon_2+\mu_1+\mu_2(1-\gamma^2)^{1/2})/(\mu_2\varepsilon_1),$$
$$c_3=(2b\beta\varepsilon_1+\varepsilon_1+\varepsilon_2+\mu_1(1-\gamma^2)^{1/2})/(\mu_2\varepsilon_1),$$
$$c_4=(1+2\beta b+\varepsilon_2(1-\gamma^2)^{1/2})/(\mu_2\varepsilon_1),\ c_5=(1-\gamma^2)^{1/2}/(\mu_2\varepsilon_1).$$

When conditions (4) are fulfilled, the studied FPL system has a synchronous mode corresponding to equilibrium state A_1. The domain of parameters C_s where conditions (4) are satisfied corresponds to the region where the synchronous mode persists.

Now let us consider the features of model (3) dynamical behavior exhibited as it parameters values lie beyond domain C_s. To this end, we analyze one-parameter bifurcation diagrams for the point mapping T_φ of the plane $\varphi=\varphi^0$ into the plane $\varphi=\varphi^0+2\pi$ produced by the trajectories of model (3). Fig.4 displays bifurcation diagram $\{b,u\}$ calculated at the parameter values γ=0.1, β=5, ε_1=1, ε_2=2, μ_1=2, μ_2=4.5, (φ, u) projections of the phase portraits, and time realizations $u(\tau)$ corresponding to the attractors of model (3).

The diagram $\{b,u\}$ (Fig.4a) characterizes evolution of quasi-synchronous mode of limit cycle S_0 (Fig.4b) as parameter b varies from −0.78 to −1.55. It shows transformation of quasi-synchronous mode into asynchronous one. As b is decreases, limit cycle S_0 is transformed into chaotic attractor P_0 through period doubling bifurcations (Figs.4c, 4d). With further decreasing of b, attractor P_0 is transformed into oscillatory-rotatory type chaotic attractor W_0 (Figs.4e, 4f). Then alternation of the attractor W_0 mode and the modes of two-turn (4π-periodic in φ) rotational limit cycles is observed. When $b<-1.363$, the system rigidly switches to the mode of one-turn rotational limit cycle L_3 (Fig.4g); then, rotatory

type chaotic attractor W_1 forms in the phase space throw period-doubling bifurcations of the limit cycle L_3 (Fig.4h). If b continues to decrease, the system passes to the oscillation mode with oscillatory-rotatory type chaotic attractor W_2 via intermittency of chaos-chaos type (Figs.4i-4l).

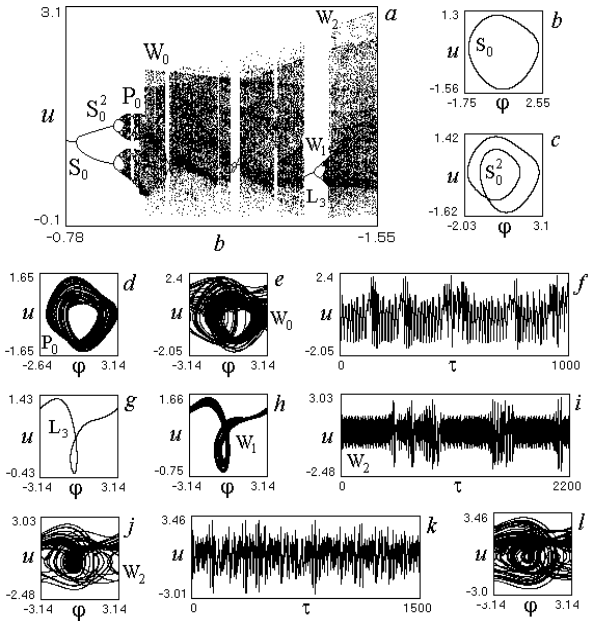

Fig. 4. Evolution of the mode of limit cycle S_0, observed as b increases (*a*), phase portraits and time realizations that correspond to attractors of system (3) for b=(*b*) –0.78, (*c*) –0.87, (*d*) –0.97, (*e,f*) –0.985, (*g*) –1.365, (*h*) –1.43, (*i,j*) –1.432, (*k,l*) –1.55

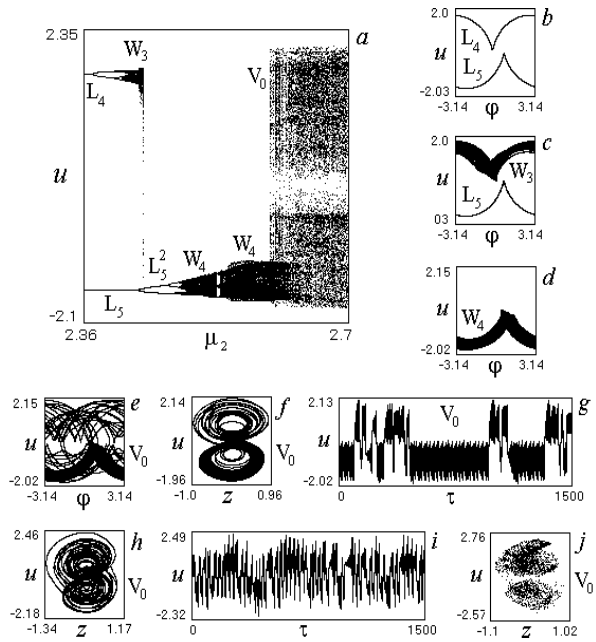

Fig. 5. Evolution of the mode of limit cycles L_4 and L_5, observed as μ_2 increases (*a*), phase portraits, Poincare cross-section, and time realizations that correspond to attractors of system (3) for μ_2=(*b*) 2.36, (*c*) 2.433, (*d*) 2.599, (*e,f,g*) 2.61, (*h,i,j*) 3.7

The model (3) exhibits such interesting phenomenon as formation of rotatory type chaotic attractor characterized by irregular switching of a phase variable u. Fig.5a represents bifurcation diagram $\{\mu_2,u\}$ corresponding to γ=0.1, b=–1.5, β=5.75, ε_1=10, ε_2=1.9, μ_1=2. It depicts formation of chaotic attractor with a variable u irregular switching on the base of rotatory type limit cycle. Figs.5b-5i show (φ,u) and (z,u) projections of the attractors' phase portraits, time realizations $u(\tau)$, and (z,u) projection of the Poincare cross-section. When μ_2=2.36, the asynchronous modes of rotational limit cycles L_4 and L_5 exist simultaneously (Fig.5b). When μ_2 increase, chaotic attractor W_3 (Fig.5c) appears in the phase space through period-doubling bifurcations for cycle L_4. Then, the system rigidly switches from the mode of attractor W_3 to the mode of two-turn rotatory type limit cycle L_5^2. After that, the mode of chaotic attractor W_4 (Fig.5d) develops as a result of period-doubling bifurcations for cycle L_5. When μ_2>2.5995, the system passes to the mode of rotational chaotic attractor V_0 with irregular variable u switching (Figs.5e, 5f, and 5g). Formation of attractor V_0 indicates that, in the phase space, there are two domains where the system chaotically oscillates and irregularly passes from one domain into the other. Figs.5h, 5i, and 5j illustrate the character of chaotic attractor V_0 observed as μ_2 increases.

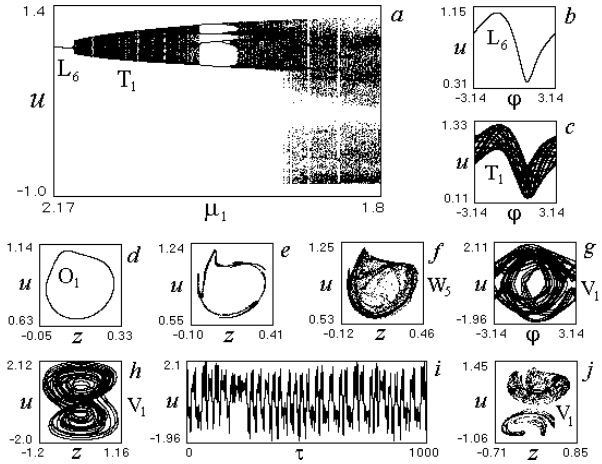

Fig. 6. . Bifurcation diagram $\{\mu_1,u\}$ (*a*), phase portraits, Poincare cross-section, and time realization that correspond to attractors of system (3) for μ_1=(*b*) 2.17, (*c,d*) 2.05, (*e*) 1.95, (*f*) 1.917, (*g,h,i,j*) 1.8

Numerical simulation shows that model (3) exhibits the loss of the stability of oscillatory and rotational limit cycles via the bifurcation of generation of stable 2D oscillatory or rotatory torus respectively in the phase space U when a pair of complex-conjugated cycle multiplicators crosses a unit circle [5]. Fig.6a represents bifurcation diagram $\{\mu_1,u\}$ corresponding to γ=0.1, b=–1.55, β=5, ε_1=1.8, ε_2=2.045, μ_2=2.35. It characterizes evolution of asynchronous mode of limit cycle L_6 when μ_1 decreases. Figs.6b-6j shows the examples of (φ,u) and (z,u) projections of attractors' phase portraits, time realization $u(\tau)$, and (z,u) projections of the Poin-

care cross-section. When μ_1 decreases, first, the mode of rotational torus T_1 (Fig.6c) appears from limit cycle L_6 (Fig.6b). After torus T_1 is formed, the phase portrait of mapping T_φ (Fig.6d) is characterized by the presence of stable closed invariant curve O_1. Then there is a "window" of values of μ_1 at the $\{\mu_1,u\}$ diagram corresponding to four-turn (8π-periodic in φ) rotational limit cycle. After this "window" the distortion of the curve O_1 is observed (Fig.6e). This phenomenon indicates gradual transformation the mode of torus T_1 to the mode of rotatory type chaotic attractor W_5 (Fig.6f). As μ_1 decrease, the mode of attractor W_5 is transformed into the mode of chaotic attractor V_1 with irregular switching of variable u (Figs.6g-6j). When μ_1<1.38, the alternation of chaos-chaos type and following transition to the mode of oscillatory torus T_0 are observed. With further decreasing of μ_1 the mode of torus T_0 mildly transforms into the quasi-synchronous mode of oscillatory type limit cycle. Therefore, the $\{\mu_1,u\}$ diagram (Fig.6a) represents an example of the system's transference from an asynchronous mode to a quasi-synchronous one.

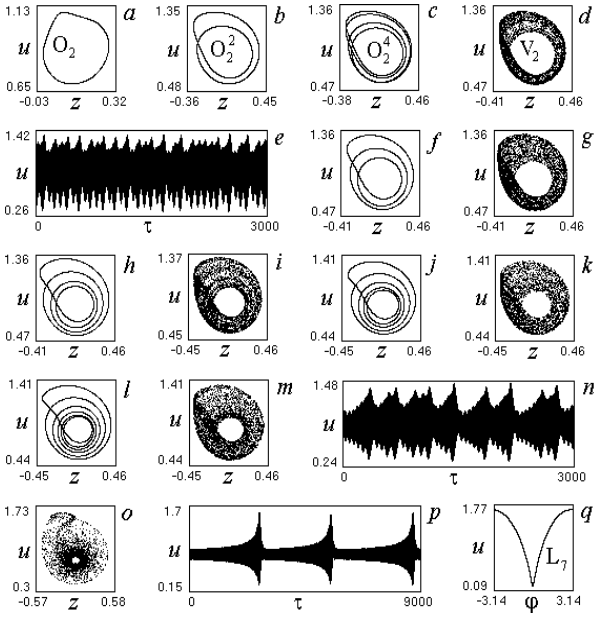

Fig. 7. Poincare cross-section, time realizations, and phase portraits corresponding to attractors of system (3) for ε_1=(*a*) 1.7, (*b*) 12.8, (*c*) 14.3, (*d,e*) 18.0, (*f*) 18.2, (*g*) 22.5, (*h*) 22.8, (*i*) 26.0, (*j*) 26.1, (*k*) 28.5, (*l*) 28.7, (*m,n*) 30.7, (*o,p*) 67.3, (*q*) 75.76

Formation of the mode of chaotic oscillations may be realized in the system considered via torus-doubling bifurcation also. Let us track the evolution of the mode of rotational torus when parameter ε_1 is varied. For this purpose, we use the numerical simulation of model (3) for γ=0.1, b=−1.55, β=5, ε_2=2.05, μ_1=2.05, μ_2=2.35. Fig.7 shows (z,u) projections of the Poincare cross-section, time realizations $u(\tau)$, and (φ,u) projection of the phase portraits corresponding to the system's attractors. Let us consider the mode of torus T_2 corresponding to close invariant curve O_2 (Fig.7a) as the system's initial state. In interval 2.12<ε_1<8.87, alternating torus T_2 and multi-turn (8π-,10π-,12π-, and 14π-periodic in φ) rotational limit cycles are observed. When ε_1>8.87, period-doubling bifurcations of curve O_2 adequate to torus-doubling bifurcations occurs (Figs.7b, 7c), and, then chaotic attractor V_2 appears (Figs.7d, 7e). If ε_1 continues to grow, the modes of attractor V_2 and of complex tori corresponding to multi-turn closed invariant curves (Figs.7f-7n) alternate. Moreover, it is found that number of turns of the closed invariant curves corresponding to these complex tori is grow one unit worth in succession; the first of these curves corresponds to three-turn torus (Fig.7f). In Figs.7f, 7h, 7j, and 7l represent three-, four-, five-, and six-turn closed invariant curves. Note, that transitions to the chaotic modes are realized via doubling of closed invariant curves. When ε_1>49.13, the stable rotational limit cycle L_7 (Fig.7q) appears in the phase space U as a result of saddle-node bifurcation. In interval 49.14<ε_1<75.51 the mode of chaotic attractor and the mode of limit cycle L_7 exist simultaneously (Figs.7o, 7p, and 7q). A still increase of ε_1 leads to rigid transition of the system from the mode of chaotic oscillations to the mode of cycle L_7 in consequence of clash the chaotic attractor and saddle rotational limit cycle in the phase space U.

Note, that described scenario of chaotization via torus-doubling bifurcations is observed in the cases when μ_2 or b are used as the control parameter.

V. Conclusion

In this paper we discussed the dynamics peculiarities of the FPL system with inverted discriminator characteristic. The obtained results show that such system exhibits a rich variety modes and complex dynamic phenomena: the loss of stability of the synchronous mode, appearance of periodic quasi-synchronous modes determined by oscillatory limit cycles of models (2) and (3), quasi-periodic quasi-synchronous and asynchronous modes corresponding to oscillatory and rotational 2D tori in the phase space, and the mode of chaotic oscillations with phase variable u irregular switching, and a transition to a chaotic asynchronous mode via the torus-doubling bifurcation. The dynamical effects and phenomena in models (2) and (3) are of fundamental importance for understanding the behavior of the system considered when the synchronous state is cut off as a result of the system parameters perturbation. The results of our analysis of the models (2) and (3) allow to make a conclusion that the FPL system with inverted frequency discriminator characteristic may be regarded as a generator of periodically and chaotically modulated oscillations.

Acknowledgements

This work was supported by the Russian Foundation for Basic Research (grants No 05-02-17409, No 06-02-16499).

References

1. V. V. Shakhgil'dyan and A. A. Lyakhovkin. Phase-Lock Systems (Svyaz', Moscow, 1972) [in Russian].
2. M. V. Kapranov. Nauch. Dokl. Vyssh. Shkoly, Radiotekh. Electron. 2 (9), p. 162 (1958).
3. V.P. Ponomarenko. Izvestiya VUZ. Applied Nonlinear Dynamics (Saratov), Vol.11, No.6. P.75 (2003).
4. L. N. Belyustina, K. G. Kiveleva, and L. A. Fraiman. Phase-Lock Systems. Ed. by V. V. Shakhgil'dyan and L. N. Belyustina (Radio i Svyaz', Moscow, 1982), p. 21 [in Russian].
5. V. S. Anishchenko. Complex Oscillation in Simple Systems (Nauka, Moscow, 1990) [in Russian].
6. V.P. Ponomarenko and V.V. Matrosov. Vestn. Verkhne-Volzhskogo otdeleniya ATN RF. Vysokie tekhnologii v radioelektronike. N. Novgorod. No. 2(4), p. 15 (1997).
7. V. P. Ponomarenko and V. D. Shalfeev. Izvestiya Vyssh. Uchebn. Zaved., Radiofizika. Vol.11. №11. P.1694 (1968).